SegDenseNet: Iris Segmentation for Pre-and-Post Cataract Surgery

Aditya Lakra*, Pavani Tripathi*, Rohit Keshari, Mayank Vatsa, and Richa Singh
IIIT-Delhi, India
Email: {aditya13006, pavani13147, rohitk, mayank, rsingh}@iiitd.ac.in

***Abstract*—Cataract is one of the major ophthalmic diseases worldwide which can potentially affect the performance of iris-based biometric systems. While existing research has shown that cataract does not have a major impact on iris recognition, our observations suggest that iris segmentation algorithms are not well equipped to handle cataract or post cataract surgery cases, thereby affecting the overall iris recognition performance. This paper presents an efficient iris segmentation algorithm with variations due to cataract and post cataract surgery. The proposed algorithm, termed as SegDenseNet, is a deep learning algorithm based on DenseNet. The experiments on the IIITD Cataract Surgery Database show that improving iris segmentation enhances the recognition performance by up to 25% across different sensors and matchers.**

I. Introduction

Iris recognition is one of the most reliable technologies available for person identification. It has gained a lot of importance due to the high accuracies and availability of commercial and open source iris recognition algorithms. Owing to the high discriminability and temporal stability of iris patterns, several large-scale systems are utilizing iris recognition systems. For instance, India's Aadhaar project [1] has enrolled over 1.2 billion citizens in the system using three biometric modalities, viz. face, fingerprint, and iris.

In existing large scale systems which include population of all age groups, several different kinds of challenges are encountered. For example, elderly population have difficulty in opening the eyes and it is difficult to ensure that young kids keep their eyes stable so that it can be captured properly. Another important covariate faced by iris recognition systems is the presence of ocular diseases. Cataract is one of the leading ophthalmic diseases in several countries. In 2010, over 800,000 cataract surgeries were performed in Germany [2] and over 81,500 in Austria [3]. In India, it has been reported that, by 2020, the Aadhaar system will have approximately $8,000,000$ cataract patients undergoing surgery annually [4]. This poses a challenge for the researchers in the biometrics field, since state-of-the-art algorithms fail to yield promising results on patients who have undergone cataract surgery [5]. To illustrate, Figure 1 shows the mis-classifications generated by commercial-off-the-shelf iris recognition systems, namely VeriEye and Matcher-1[1]. The current recommendations include that the individuals have to be re-enrolled into the system a few weeks after the surgery [1], [5]. This implies that approximately 8 million citizens will have to be re-enrolled annually by 2020. Since re-enrollment is a manually expensive task, this research explores an alternative strategy to improve the performance of iris recognition.

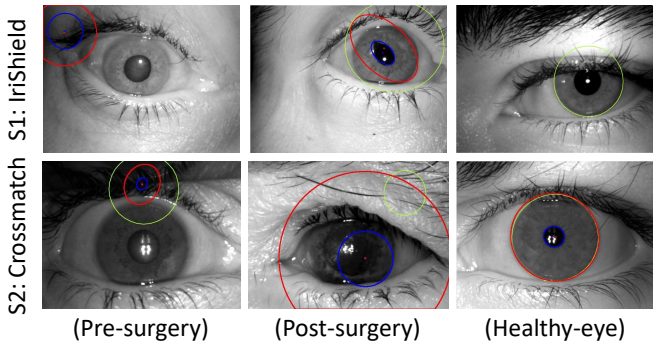

Fig. 1: Illustrating the challenges associated with iris segmentation of cataract affected eyes. Two commercial-of-the-shelf (COTS) systems have been used to segment the cataract affected iris images. Green and red & blue circles represent segmentation using VeriEye and Matcher-1, respectively.

Researchers have made significant efforts in studying the effect of cataract surgery on the iris pattern and structure. Roizenblatt *et al.* [6] were the first one to study the consequences of cataract surgery on iris pattern. Their hypothesis was that iris recognition systems fail due to changes such as depigmentation and localized iris atrophy, with loss of large areas of Fuchs crypts, circular, and radial furrows and pupil ovalization. However, Dhir *et al.* [7] performed a study on a small dataset of 15 subjects and concluded that cataract surgery does not affect iris patterns; rather, dilation of pupil and specular reflections in the pupil region are the reasons why conventional circle-based algorithms and light-position-based pupil segmentation algorithms fail to achieve high accuracy. Recently, Preethi and Jayanthi [8] have observed that structural changes occur in iris. Therefore, it is advisable to re-enroll a patient after surgery. Nigam *et al.* [9] have also shown that, in case of different ophthalmic diseases, incorrect segmentation of iris region is a potential cause of reduced accuracy of state-of-the-art iris recognition systems. Thus, it is imperative to improve the existing algorithms to ensure accurate segmentation of the iris regions in pre-and-post cataract surgery images.

To the best of authors' knowledge, existing literature on iris

*Equal contribution by student authors
[1]Due to license restriction, we cannot name the Matcher-1.

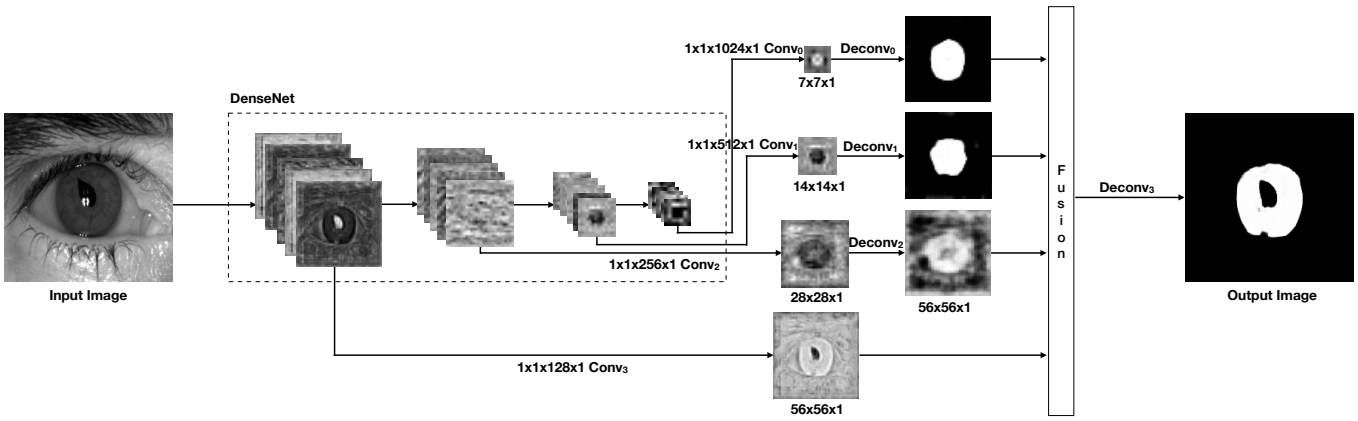

Fig. 2: Architecture of the proposed iris segmentation algorithm.

segmentation does not discuss pre-and-post cataract surgery images. There are few algorithms which present iris segmentation algorithm under unconstrained environment. For example, Zhao and Kumar [10] have proposed a method which segments the iris region based on the pupillary and limbic regions as well as by fitting a parabolic equation around the eyelids. Liu *et al.* [11] have proposed a deep learning based architecture for iris segmentation. The model yields state-of-the-art accuracy on CASIA v4-Distance and UBIRISv2 datasets and does not require post-processing. Recently, Jalilian *et al.* [12] have proposed linear and non-linear domain adaptation methods for iris segmentation using fully convolutional network.

This research focuses on a unique challenge of iris recognition: processing pre-and-post cataract surgery iris (eye) images. As mentioned earlier, we have observed that pre-and-post cataract surgery stages affect iris segmentation (Figure 1). Therefore, to address these variations, we propose a novel deep learning based segmentation algorithm, termed as SegDenseNet. The proposed data driven approach learns the variations due to pre-and-post cataract surgery and provides non-linear segmentation boundaries. The paper also presents IIIT-D Cataract Surgery Database along with annotated segmentation ground truth. The database has images pertaining to 132 subjects acquired using three different sensors, namely Crossmatch, IriShield, and Vista. Experiments show that the proposed segmentation algorithm is able to accurately segment iris and pupil boundaries in both pre-and-post cataract surgery images.

II. SegDenseNet: Iris Segmentation Algorithm

Inspired by the success of convolutional neural networks, researchers have explored their effectiveness for segmenting natural images. Long *et al.* [13] have modeled segmentation as a classification problem and designed Fully Convolutional Networks (FCN) for semantic segmentation. FCN is a special kind of neural network which only has convolution layers, pooling layers, and up-sampling layers. It can input an arbitrary sized image and output a mask of corresponding size. Chen *et al.* [14] have used ResNet [15] architecture and shown that with deep architectures, semantic segmentation accuracy can be improved significantly. Drozdzal *et al.* [16] have proposed a deep learning based architecture for semantic segmentation using DenseNet [17] and demonstrated that deep architecture indeed increases the segmentation accuracy.

Unlike segmentation in natural images, iris segmentation is somewhat different. While semantic segmentation requires global as well as local information, iris segmentation requires very fine details such as inclusion of iris features, sharp boundary of the iris, and disposing the fine iris regions occluded by reflection, eye-lash and hair. Moreover, during cataract, a cloudy white layer forms on the pupil, due to which state-of-the-art iris segmentation algorithms which use pixel intensity values to segment the iris fail to segment the correct region of interest. In post cataract surgery, the specular reflections due to implanted lens and morphological changes on the iris and pupil increase the failure cases.

Inspired from the concept of FCN [13], we propose SegDenseNet for cataract affected iris segmentation which fuses the outputs from all the convolution blocks present in a deep learning architecture. Figure 2 shows the architecture of the proposed SegDenseNet. In the proposed architecture, we have used DenseNet [17] with 121 convolution layers, with four convolution blocks. For fine predictions of the iris region, outputs from all the four dense blocks are fused.

As illustrated in Figure 2, because there is only one class (the iris region), the number of channels in the mask is one. As shown in Eqs. 1-3, the channel dimension of the outputs of three DenseNet blocks is reduced to 1 using convolution and then deconvolved to produce feature maps with coarse and fine details of the iris region. The output of the first block, represented by Eq. 4, is directly fused after channel reduction of the feature maps with other deconvolved outputs. In the proposed architecture, the fusion layer performs a weighted sum operation on the four prediction maps (Eq. 5). For our experiments, all the intermediate feature maps have been given equal weights. Finally, the fused output is deconvolved to the size of the input image, to produce the desired mask (Eq.

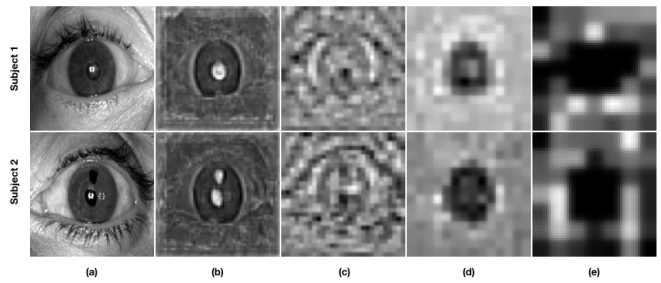

Fig. 3: Outputs of the four convolution blocks used for fusion. (a) Input image. Sample output of (b) first convolution block, (c) second convolution block, (d) third convolution block and (e) fourth convolution block

6). The sample outputs of the four convolutional blocks before they are converted to feature maps with 1 channel are visualized in Figure 3.

$$I_1 = Df_n(X'_{N'}) \otimes Conv_0(1,1,1)\Psi Deconv_0(4,4,1) \quad (1)$$

$$I_2 = Df_n(X'_{(N'-1)}) \otimes Conv_1(1,1,1)\Psi Deconv_1(8,8,1) \quad (2)$$

$$I_3 = Df_n(X'_{(N'-2)}) \otimes Conv_2(1,1,1)\Psi Deconv_2(16,16,1) \quad (3)$$

$$I_4 = Df_n(X'_{(N'-3)}) \otimes Conv_3(1,1,1) \quad (4)$$

$$I_5 = w_1 I_1 + w_2 I_2 + w_3 I_3 + w_4 I_4 \quad (5)$$

$$M = Df_n(I_5)\Psi Deconv_3(8,8,1) \quad (6)$$

Pseudo code of the proposed SegDenseNet is given in Algorithm 1. The datasets A and B represent CASIA v4-Distance and IIITD Cataract Surgery databases, respectively. X_N^{tr} depicts the training set which contains the images of dimension 224×224 and associated and labels. The DenseNet-121 model, pretrained on ImageNet dataset, is modified according to iris segmentation. The images are first resized and then augmented. Post augmentation, we train the network in a batch mode. During testing, the predicted mask is generated. We binarize the predicted masks and resize them to the size of the original image i.e. 640×480. The error is then computed between the ground truth mask, $M_G^{te'}$ and predicted mask, $M_P^{te'}$.

III. Database and Experimental Protocol

The performance of the proposed iris segmentation algorithm is demonstrated on the IIIT-D Cataract Surgery database. Since the cataract database is small in size, CASIA v4-Distance database is used for training *iris specific features*. In the following subsections, we describe the dataset details, experimental protocol, and the implementation details.

Algorithm 1 Cataract Iris Segmentation

Database: {A, B}
Input: $X_N^{tr} \leftarrow$ {A, B}; $X_P^{te} \leftarrow$ {B}
Output: M_P^{te}
Model: $SDM \leftarrow SegDenseNet(DenseNet-121)$
$X_N^{tr'} \leftarrow resize(X_N^{tr})$
$X_{N'}^{tr'} \leftarrow augment(X_N^{tr'})$
for Batch in $X_{N'}^{tr'}$ **do**
    $train(SDM(Batch))$
end for
for Batch in X_P^{te} **do**
    $M_P^{te} \leftarrow test(SDM(Batch))$
end for
Post-processing: $M_P^{te'} \leftarrow resize(Binarize(M_P^{te}))$
$error = \frac{1}{P \times m \times n} \sum_{i,j \epsilon (m,n)} M_G^{te'}(i,j) \bigoplus M_P^{te'}(i,j)$

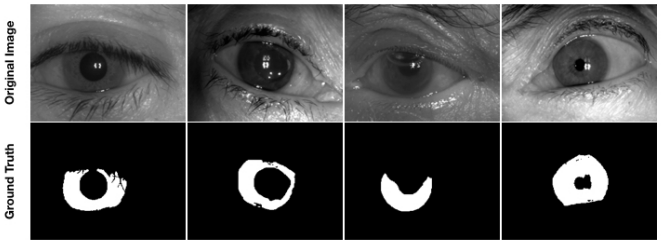

Fig. 4: Sample iris images and their manually generated ground truth masks.

A. Datasets

CASIA v4-Distance database [18] contains 2567 face images pertaining to 142 different subjects in the NIR spectrum. Since the images are captured from a distance, all the images have some level of noise. Each image captures a large portion of the whole face thus containing both the irises of the subject. After segmenting the eye region of these images, both right and left eye images are used for pre-training.

IIITD Cataract Surgery Database[2] contains eye images from 132 subjects. In total, there are 764 pre-surgery and 764 pre-surgery images. However, the database only contains the class labels and not the segmentation annotations. To evaluate the segmentation performance, we manually annotated a total of 904 ground truth masks. Figure 4 shows some of the input images and their corresponding annotations. It can be observed visually how sharp, fine and accurate the ground truth masks are. These annotations will be publicly available to the research community[3]. 70% database is utilized for training and the remaining 30% images (from unseen subjects) are used for evaluating the segmentation performance. The original size of the images is 640×480, however, the experiments are performed with images resized to 224×224.

[2]http://iab-rubric.org/resources/ICSD.html
[3]http://www.iab-rubric.org/resources.html

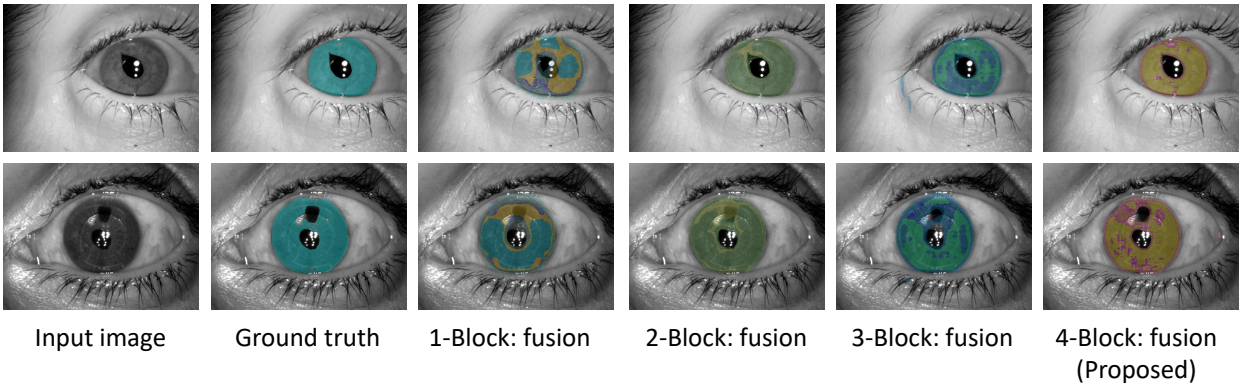

Fig. 5: Visual illustration of the effect of fusing different number of dense blocks on the segmentation performance (obtained masks are superimposed on the original image). The two colors in the masks represent high and low confidence levels.

B. Implementation Details

The proposed deep learning architecture has been implemented in Keras [19] with Tensorflow backend. The DenseNet-121 model pretrained on imagenet is first trained using left and right healthy iris images from the CASIA v4-Distance dataset [18], followed by finetuning using IIITD Cataract Surgery Database. While training the model, the learning rate and momentum values are set as 0.001 and 0.9 respectively with SGD optimizer. The model was trained on NVIDIA GTX 1080ti GPU for a total of 500 epochs. Since deep learning architectures require large number of samples for training, images from both the datasets, CASIA v4-Distance [18] and IIITD Cataract Surgery Databases, are used to augment the training database. The database is further augmented using contrast normalization and flip operations to increase the database size by 10 times. For contrast normalization, we have used 4 different contrast factors where contrast factor is the number of times by which the difference between a pixel value and the center value has to be multiplied.

C. Fusion of Dense-blocks

In our implementation, we have used DenseNet-121 which has four convolution blocks. Through visualization of masks, as depicted in Figure 5 it can be inferred that fusion of four blocks gives the best result. The two cases presented in the Figure 5 showcase the morphological changes that may occur post cataract surgery. The first row represents a case of pupil rupture. The protrusion in the pupil is completely segmented out only by the proposed method. In the case of the patient in second row, the surgery has resulted in a puncture inside the iris region. This deformity is completely segmented as non-iris region only when four Dense-blocks are fused. While in the other cases, some part of the puncture is segmented as iris region with low confidence.

IV. Experimental Results and Analysis

The performance of the proposed algorithm is evaluated in terms of both segmentation and matching performance. For segmentation, the results are compared with Zhao and Kumar [10], while the impact of the segmentation algorithm on matching is demonstrated using a commercial system and the deep learning based algorithm by Zhao and Kumar [20].

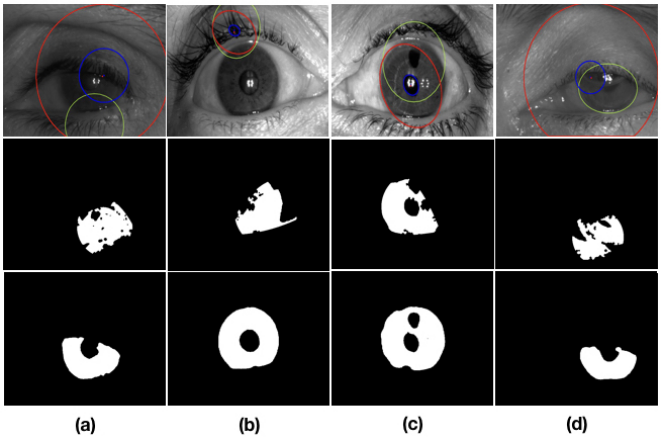

Fig. 6: Showcasing the results of iris segmentation on pre (a)-(b) and post (c)-(d) cataract surgery images. First row shows the segmentation results using COTS, second row shows results of Zhao and Kumar [10], and the last row pertains to the masks predicted using the proposed algorithm.

TABLE I: Average segmentation error rates on IIITD Cataract Surgery Database.

Method	Error (%)
Proposed Method	0.98
Zhao and Kumar [10]	6.28

Segmentation Performance: The performance of the segmentation algorithm is measured in terms of metric from NICE-I competition [21]. The average classification error rate is calculated using equation 7.

$$Error = \frac{1}{N \times m \times n} \sum_{i,j=1}^{m,n} M_G^{te'}(i,j) \oplus M_P^{te'}(i,j) \qquad (7)$$

In Eq. 7, N, m and n denote the total number of test samples,

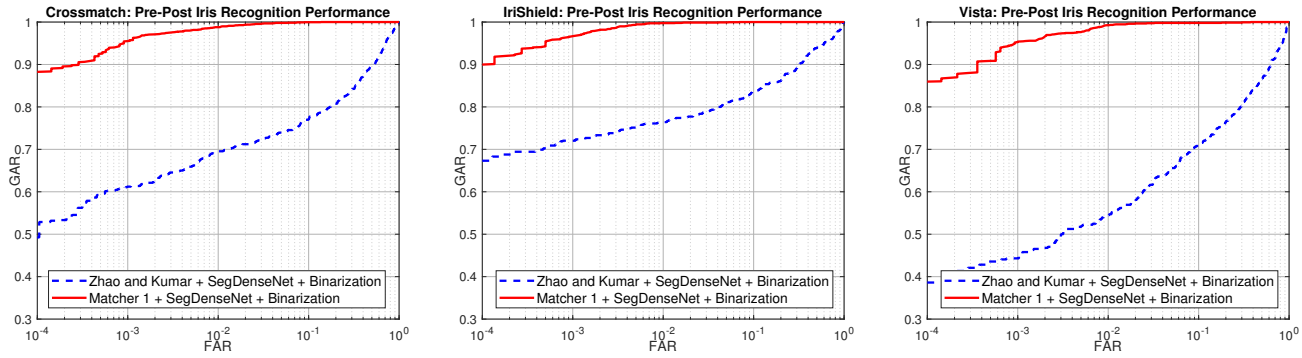

Fig. 7: ROC curves of the recognition experiments performed on pre-post cataract surgery images.

TABLE II: Comparing verification accuracies at 0.1% false accept rate on the IIITD Cataract Surgery database.

Sensor	Experiment	Subjects	Pre-Pre (%)	Post-Post (%)	Pre-Post (%)
CrossMatch	Matcher-1	44	97.1	76.5	68.2
	Matcher-1 + SegDenseNet		99.3	84.7	92.1
	Matcher-1 + SegDenseNet + Post-processing		99.5	86.8	**95.6**
	Zhao and Kumar [10], [20]		43.1	64.1	25.2
	Zhao and Kumar [20] + SegDenseNet		80.7	78.0	56.8
	Zhao and Kumar [20] + SegDenseNet + Post-processing		89.8	70.7	61.2
IriShield	Matcher-1	39	97.4	81.1	73.7
	Matcher-1 + SegDenseNet		99.6	92.5	95.5
	Matcher-1 + SegDenseNet + Post-processing		99.6	93.2	**96.7**
	Zhao and Kumar [10], [20]		78.6	89.7	56.9
	Zhao and Kumar [20] + SegDenseNet		95.3	85.7	72.4
	Zhao and Kumar [20] + SegDenseNet + Post-processing		95.2	83.1	72.0
Vista	Matcher-1	27	96.8	83.7	75.0
	Matcher-1 + SegDenseNet		99.2	92.9	90.9
	Matcher-1 + SegDenseNet + Post-processing		99.4	94.1	**95.4**
	Zhao and Kumar [10], [20]		3.4	5.4	0.7
	Zhao and Kumar [20] + SegDenseNet		91.4	69.0	43.1
	Zhao and Kumar [20] + SegDenseNet + Post-processing		90.1	75.5	44.3

height of the mask, and width of the mask, respectively. The logical exclusive-or operator calculates the proportion of the correspondent disagreeing pixels.

Figure 6 shows failed cases of COTS system. The results obtained using state-of-the-art iris segmentation technique proposed by Zhao and Kumar [10] are also shown in the figure along with the iris masks obtained using SegDenseNet. It should be noted that Zhao and Kumar's method involves parameter tuning. We have tried to fine-tune the parameters to the best of our ability. It achieves average segmentation error of 6.28% after parameter tuning. The proposed deep learning based segmentation algorithm yields 0.98% average segmentation error. The average segmentation error for both the algorithms are compiled in Table I.

Recognition Performance: For calculating the iris recognition accuracy, we have used a state-of-the-art commercial software (Matcher-1) and Zhao and Kumar's [20] state-of-the-art deep learning based iris recognition algorithm. Table II summarizes the recognition accuracies obtained with and without the proposed segmentation algorithm, SegDenseNet.

The matching is performed amongst images captured before surgery (Pre-Pre), after surgery (Post-Post), and between images captured before and after surgery (Pre-Post). The recognition accuracies are summarized in Table II. It can be observed that there is a significant rise in the accuracies when SegDenseNet is used. For instance, with the COTS recognition pipeline, incorporating SegDenseNet improved the accuracies by 2.4%, 2.2%, and 2.6%, in case of Pre-Pre matching while using the three sensors, namely Crossmatch, IriShield and Vista, respectively. In case of Post-Post we have achieved 10.3%, 12.1% and 10.4% increase in accuracies and in Pre-Post case the accuracies are improved by 27.4%, 23.0% and 20.4% for the three sensors, respectively. Similar trend in the results are observed when Zhao and Kumar's [20] recognition pipeline was used. However, the accuracies were not as high as those obtained using COTS system. This could be because none of the publicly available models are trained using the cataract dataset. Also, due to failure to process, six images were removed from the testing set. The ROC curves in Figure 7 compare the recognition accuracies obtained by Matcher-1 and Zhao and Kumar's [20] recognition pipeline when they are used with our proposed segmentation technique, SegDenseNet.

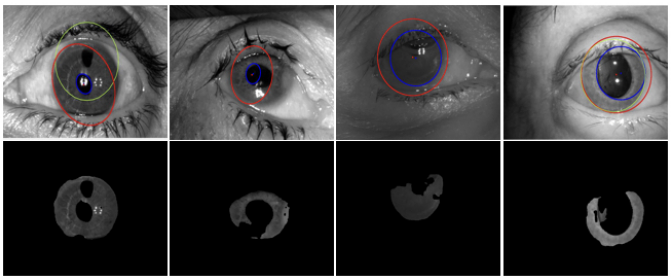

Fig. 8: Sample cases where COTS as well as the proposed method failed to segment the iris properly. Green and Red & Blue circles represent output of VeriEye and Matcher-1 respectively.

Figure 8 shows exemplars of images where the proposed algorithm and commercial SDKs failed to correctly segment out the iris region. On visually observing the images, we concluded that the failure happens due to bubbles in eyes. Also, in most of the failed cases, iris images are present at off-angle while there are very few training samples with off-angle iris region and/or bubbles. It is our assertion that if the model is trained with more number of such data samples, then the model should be able to successfully segment the iris region.

V. Conclusion

Cataract and it's post-operative complications can cause iris recognition algorithms to fail, particularly at the segmentation stage. Irregular pupil shape and significant specular reflections after surgery are primary reasons for these segmentation failures. Therefore, this research focuses on designing a segmentation algorithm for extracting iris region from eyes with cataract and post cataract surgery. We propose a deep learning based segmentation algorithm, named as SegDenseNet, that utilizes four dense blocks to learn model-specific iris shape even in presence of irregularities. Segmentation results on IIITD Cataract Surgery Database show that the proposed deep learning based segmentation algorithm outperforms existing segmentation algorithms for cataract affected eyes. The matching results also demonstrate the importance of improving the segmentation algorithms on the cataract and post-operative cases. As future work, we plan to work on designing segmentation algorithm that effectively segments iris images in presence of multiple kinds of covariates such as distance, occlusion, and alcohol [22].

VI. Acknowledgement

This research is partly supported through a grant from MEITY. R. Keshari is partially supported by Visvesvaraya Ph.D. fellowship. M. Vatsa and R. Singh are partially supported through Infosys Center for Artificial Intelligence, IIIT-Delhi, India.

References

[1] "Unique *i*dentification *a*uthority of *i*ndia." [Online]. Available: https://uidai.gov.in

[2] T. Kohnen, M. Baumeister, D. Kook, O. K. Klaproth, and C. Ohrloff, "Cataract surgery with implantation of an artificial lens," *DAI*, vol. 106, no. 43, pp. 695–702, 2009.

[3] "Statistics austria - annual national health report from statistics austria," Tech. Rep. 76, 2012.

[4] M. Gudlavalleti, S. Gupta, N. John, and P. Vashist, "Current status of cataract blindness and vision 2020: The right to sight initiative in india," vol. 56, pp. 489–94, 2008.

[5] O. Seyeddain, H. Kraker, A. Redlberger, A. Dexl, G. Grabner, and M. Emesz, "Reliability of automatic biometric iris recognition after phacoemulsification or drug-induced pupil dilation," vol. 24, p. 0, 2013.

[6] R. Roizenblatt, P. Schor, F. Dante, J. Roizenblatt, and R. Belfort, "Iris recognition as a biometric method after cataract surgery," *BEO*, vol. 3, no. 1, 2004.

[7] L. Dhir, N. E Habib, D. M Monro, and S. Rakshit, "Effect of cataract surgery and pupil dilation on iris pattern recognition for personal authentication," vol. 24, pp. 1006–10, 2009.

[8] D. Preethi and V. Jayanthi, "SOM clustering approach: investigation on cataract surgery structural changes in iris," *Biomedical Research*, vol. 28, no. 12, 2017.

[9] I. Nigam, M. Vatsa, and R. Singh, "Ocular biometrics: A survey of modalities and fusion approaches," *Information Fusion*, vol. 26, pp. 1–35, 2015.

[10] Z. Zhao and A. Kumar, "An accurate iris segmentation framework under relaxed imaging constraints using total variation model," in *IEEE ICCV*, 2015.

[11] N. Liu, H. Li, M. Zhang, J. Liu, Z. Sun, and T. Tan, "Accurate iris segmentation in non-cooperative environments using fully convolutional networks," in *IEEE ICB*, 2016.

[12] E. Jalilian, A. Uhl, and R. Kwitt, "Domain adaptation for cnn based iris segmentation," in *BIOSIG*, 2017.

[13] J. Long, E. Shelhamer, and T. Darrell, "Fully convolutional networks for semantic segmentation," *CoRR*, vol. abs/1411.4038, 2014.

[14] L. Chen, G. Papandreou, I. Kokkinos, K. Murphy, and A. L. Yuille, "Deeplab: Semantic image segmentation with deep convolutional nets, atrous convolution, and fully connected crfs," *CoRR*, vol. abs/1606.00915, 2016.

[15] K. He, X. Zhang, S. Ren, and J. Sun, "Deep residual learning for image recognition," in *IEEE CVPR*, 2016, pp. 770–778.

[16] S. Jégou, M. Drozdzal, D. Vázquez, A. Romero, and Y. Bengio, "The one hundred layers tiramisu: Fully convolutional densenets for semantic segmentation," *CoRR*, vol. abs/1611.09326, 2016.

[17] G. Huang, Z. Liu, and K. Q. Weinberger, "Densely connected convolutional networks," *IEEE CVPR*, 2017.

[18] "Biometrics ideal test," *http://biometrics.idealtest.org/dbDetailForUser.do?id=4*.

[19] F. Chollet, "keras," https://github.com/fchollet/keras, 2015.

[20] Z. Zhao and A. Kumar, "Towards more accurate iris recognition using deeply learned spatially corresponding features," in *IEEE ICCV*, 2017.

[21] "NICE-I - noisy iris challenge evaluation - part i," *http://nice1.di.ubi.pt/index.html*, 2009.

[22] S. S. Arora, M. Vatsa, R. Singh, and A. Jain, "Iris recognition under alcohol influence: A preliminary study," in *IAPR International Conference on Biometrics*, 2012, pp. 336–341.